Colloids and Surfaces B: Biointerfaces 140 (2016) 254–261

Contents lists available at ScienceDirect

Colloids and Surfaces B: Biointerfaces

journal homepage: www.elsevier.com/locate/colsurfb

Coating morphology and surface composition of acrylic terpolymers with pendant catechol, OEG and perfluoroalkyl groups in varying ratio and the effect on protein adsorption

Jun Zhong [a,*], Hua Ji [a,b], Jiang Duan [b], Haiyang Tu [b], Aidong Zhang [b,*]

[a] Orthopaedic Department of Renmin Hospital, Wuhan University, Wuhan 430060, PR China
[b] Key Laboratory of Pesticide and Chemical Biology of Ministry of Education, Central China Normal University, Wuhan 430079, PR China

ARTICLE INFO

Article history:
Received 20 August 2015
Received in revised form 3 December 2015
Accepted 27 December 2015
Available online 31 December 2015

Keywords:
Protein adsorption
Antifouling
Terpolymer
Morphology
Perfluoroalkyl
Poly(ethylene glycol)
Catechol
Dopamine

ABSTRACT

This work aims at developing versatile low-biofouling polymeric coatings by using acrylic terpolymers (DOFs) that bear pendant catechol (D), oligo(ethylene glycol) (O), and perfluoroalkyl (F) groups in varying ratios. The polymers were endowed with the ability to form firmly coatings on virtually any surfaces and undergo surface microphase separation and self-assembly, as revealed by the surface enrichment of F pendants and the morphology variation from irregular solid domains to discrete crater-type aggregates of different size. The effect on protein adsorption was investigated using bovine serum albumin (BSA) and adhesive fibrinogen (Fib) as model proteins. The coating of DOF164 (low F content), which has morphology of discrete crater-type aggregates of ~400 nm in size, adsorbed a least amount of protein but with a highest protein unit activity as determined by SPR and immunosorbent assay; whereas the coating of DOF1612 (high F content) showed a 12.3-fold higher adsorption capacity toward Fib. Interestingly, a 2.2-fold lower adsorption amount but with a 1.8-fold higher unit activity was found for Fib adsorbed on the DOF164 surface than on DOF250 (without F fraction), whose OEG segments being a widely recognized protein compatible material. The features of the DOF164 terpolymer presenting a robust coating ability and a minimal protein adsorption capacity while with a high protein unit activity suggest its potential application as a non-fouling surface-modifier for medical antifouling coatings and as a matrix material for selective protein immobilization and activity preservation in biosensor construction.

1. Introduction

Antifouling of solid surfaces is of great importance in the fields of biotechnology, biomedicine and materials science [1]. Implantable medical devices, such as catheters, and contact lenses, along with cell culture substrates and biosensors, rely on a level of protection against biofouling [2,3]. The accumulated knowledge indicates that the antifouling effect can be realized through either hydrophilic or hydrophobic coatings, and improved greatly by using the coatings of polymers bearing mixed hydrophilic/hydrophobic segments at an optimum ratio [4,5]. Recent investigations revealed that coating topography also plays an important role in repelling biospecies adsorption [6]. Essentially, the chemistry and morphology of a surface are the two determinants, forming the basis for numerous strategies to construct surface coatings with desired antifouling properties. Despite the great efforts to date, developing amphiphilic copolymers that are able to form robust coatings with simple procedures on any surface to give excellent antifouling properties still remains a great challenge.

The surface chemistry in antifouling coatings is the chemical constitution capable of repelling adsorption of proteins and organisms. Various polymers bearing both hydrophilic and hydrophobic chains, with which to form coatings generally termed as amphiphilic surfaces, have proven to be effective [7]. The functionalities, such as length-varying poly(ethylene glycol) (PEG) [8], zwitterionic group [9], dextran [10], perfluoroalkyl (PFA) [11], and polydimethylsilicone [12], etc., have frequently been used for elaborating amphiphilic polymers. The compositional ratio of the respective segments in polymer has great effect on the coating antifouling property. In general, a maximum resistance to protein adsorption can be found when a polymer surface is composed of hydrophilic and hydrophobic segments in an appropriate ratio [13]. Moreover, for a polymer coating with fluorine-containing

* Corresponding authors.
E-mail addresses: zhongjun8496@aliyun.com (J. Zhong), adzhang@mail.ccnu.edu.cn (A. Zhang).

http://dx.doi.org/10.1016/j.colsurfb.2015.12.051
0927-7765/

segments, the interface reconstruction induced by migration and exposure of fluorinated segments to the air/polymer interface can improve greatly the antifouling effect [14]. One less studied aspect is the morphology variation induced by the self-assembly of amphiphilic copolymer coatings and the effect on antifouling, and sometimes this morphology variation has a significant role in reducing biofouling [15]. However, it is usually not easy to predict and/or control the self-assembly morphology of an amphiphilic polymer and the effect on antifouling. Therefore, more knowledge is highly demanded in design of new antifouling polymeric coating materials.

Another challenge for amphiphilic polymer coatings is their weak adhesion on surface due to their amphiphilic nature. To address this issue, some strategies have been devised to improve adhesion, for example, using the well-known covalent "graft-to" and "graft-from" methodologies to construct robust amphiphilic polymer coatings [16,17]. In recent years, catechol-containing polymeric coatings, inspired by the mussel foot adhesive proteins, have attracted great attention owing to the universal adhesion ability on virtually any surface [18]. By incorporation with conventional hydrophilic components such as poly(ethylene oxide) [19], hyperbranched polyglycerol [20], heparin [21], and even hydrophobic perfluoroalkyl group [22], the catechol-containing coatings have been demonstrated to achieve long-term stability and antifouling performance. In general, an optimum amount of catechol units in a polymer chain is necessary to form a stable coating via anchoring and crosslinking, and more interestingly, to aggregate and form nanoparticle-like structures on surface [23]. Although model surfaces composed of the PEG and PFA segments have been frequently employed in elaborating amphiphilic antifouling polymers [7,13], catechol-containing fluorinated amphiphlic copolymers have not been explored so far.

We envisioned that if catechol could be incorporated into the amphiphilic copolymer comprising of OEG and PFA segments, there may be two advantages for the coatings: one is the robustness of the resultant coatings through catechol anchoring; the other is the ability to control the morphology via interfacial reorganization of the OEG and PFA segments and inter-chain cross-linking of the catechol units. Thus in the present work a series of catechol-containing acrylic copolymers were synthesized with the combination of three monomers *N*-(3,4-dihydroxyphenylpropyl) methacrylamide (DMA, D), oligomeric ethylene glycol methacrylate (OEG, O), and perfluorohexylethyl acrylate (PFA, F) in varying ratios (Scheme 1). The copolymers were spin- or dip-coated on gold, silicon and stainless steel surfaces for assessing their surface morphology and antifouling properties. We anticipated that the combination of amphiphilicity with adhesive functionality would endow the coatings with the desired antifouling properties and coating robustness on virtually any surface.

2. Experimental

2.1. Materials

3,4-Dihydroxyphenylalanine hydrochloride (dopamine·HCl), 2,2′-azodiisobutyronitrile (AIBN), 2-(perfluorohexyl) ethyl acrylate (PFA, F), olige(ethylene glycol) methyl ether methacrylate (OEG, O), fibrinogen (Fib), fluorescent labled fibrinogen (FITC-Fib), and bovine serum albumin (BSA) were purchased from Sigma Aldrich. All the used proteins were dissolved in PBS buffer (pH 7.4) at a concentration of 1 mg/ml. Methacryloyl chloride was purchased from Wuhan Shenshi chemical reagents company (China). Fib enzyme-linked immunosorbent assay (ELISA) kit was purchased from R&D Systems, Inc. All other reagents were purchased of the highest purity.

Table 1
Composition and molecular weight of polymers DOF.

Polymer	Monomer ratio (mol%)[a]			Molecular weight[b]		
	D	O	F	Mw	Mn	PDI
DOF250	28.6	71.4	0	16130	7260	2.22
DOF495	22.2	50	27.8	15580	7130	2.16
DOF164	9.1	54.5	36.4	19680	7690	2.56
DOF1612	5.3	31.6	63.1	17520	5650	3.10

[a] Monomer composition based on ^{1}H NMR analysis.
[b] Molecular weight by GPC using polystyrene standard (THF eluent).

2.2. Synthesis of polymers

The catechol-containing methacrylamide (DMA, D) was synthesized according to the literature [24]. The copolymers were prepared via the random free radical polymerization of the three respective monomers (D, O, and F) in varying ratios (Scheme 1 and Table 1). The total amount of monomers was kept constant at 10 mmol and the molar percentage of AIBN fixed at 10%. All monomers (typically 221–552.5 mg for D, 900–2490 mg for O, and 0–2633 mg for F) were dissolved in DMF (15 mL), and then AIBN (164 mg, 1 mmol) was added. The solution was heated at 65 °C overnight under nitrogen. Then the reaction mixture was added 20 mL of dichloromethane and washed with saturated brine (20 mL × 3). The organic phase was added diethyl ether (400 mL) and the polymer precipitated. The precipitate was re-dissolved in dichloromethane and precipitated again with diethyl ether. The molecular weights were determined by gel permeation chromatography (GPC), and their structures were characterized by ^{1}H NMR spectroscopy and FT–IR spectroscopy. The general structure of the polymers is presented as DOFxyz in which the footnote xyz represents the compositional molar ratio of the respective monomers.

2.3. Surface preparation and characterization

Substrates of glass coated with evaporated gold film (standard SPR gold film chips used with the SPR instrument mentioned below, having an evaporated gold film thickness of 50 nm on quartz) were immersed with 20% H_2O_2, 1% $NaBH_4$ aqueous solution in sequence, followed by water rinsing and cleaning with H_2 plasma in a Harrick Plasma Cleaner (Sterilizer PDG-32G) for 10 min. The stainless steel and silicon substrates were ultrasonic cleaned in isopropanol and double-distilled water for 10 min, then treated with H_2 plasma. The substrates were spin-coated (low speed 500 r/min, 12 s; high speed 1000 r/min, 60 s) or dip-coated using the polymer solution (1 mg/mL in THF), thereafter rinsed with ethanol and dried with nitrogen stream.

The static contact angles on the coated or non-coated glass surfaces were measured by a contact angle system OCA 20 (Dataphysics, Germany) at room temperature using deionized water (1.0 μL) and methylene iodide (1.0 μL). The surface energies were derived using the Young–Good–Girifalco–Fowkes equation in the associated software. For each polymer coating sample, 5–10 measurements from different spots on the same surface were done and the average values are presented.

Grazing incidence infrared spectra (GIR) were acquired using a Tensor 27 FTIR spectrometer equipped with a microscope Hyperion 2000, a grazing angle objective (Bruker Optics), and a liquid nitrogen cooled MCT detector. The measurements were performed with 1000 co-addition scans at a spectral resolution of 4 cm^{-1}.

X-ray photoelectron spectroscopy (XPS) measurements were carried out on a VG Multilab 2000 XPS spectrometer with an Al Ka X-ray source. The energy scale was referenced to the Au 4f7/2 peak of copolymer-coated gold at a binding energy (BE) of 84.0 eV.

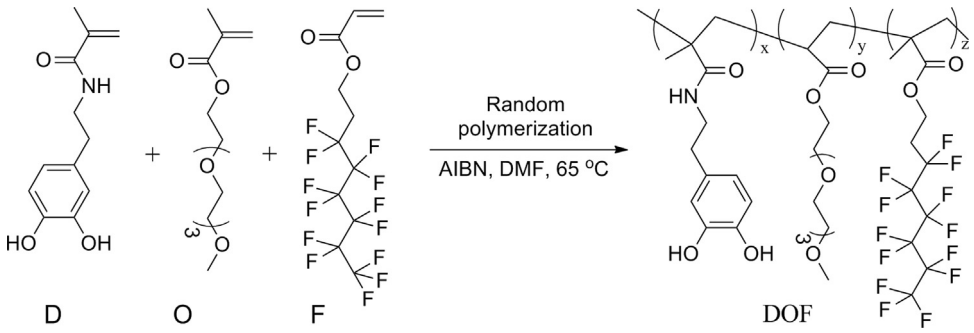

Scheme 1. Synthesis of DOF copolymers.

Morphologic images of coatings on silicon wafers were acquired using a Bruker's MultiMode-8 SPM atomic force microscope (AFM) system with a silicon cantilever in tapping mode in an area of $5 \times 5\,\mu m$ under ambient conditions. A typical force constant $0.12\,N\,m^{-1}$ and a scanning rate 0.977 Hz were used. AFM raw data were processed by the associated software NanoScope Analysis, Bruker.

2.4. Protein adsorption assay

Protein adsorption on the DOF surfaces was measured with an Autolab SPRINGLE surface plasmon resonance (SPR) system (Echo Chemie B.V., the Netherlands). The instrumental setup is based on the Kretschmann configuration with a monochouromatic p-polarized laser ($\lambda = 670\,nm$) as the light source. A DOF-coated sensor chip was mounted in the flow cell and measurement performed with a fixed liquid flow rate of 50 μL/min. After a stable baseline was achieved using a flow of phosphate buffer solution (PBS, pH 7.4), the protein solution at a concentration of 1 mg/mL in the same buffer was allowed to flow for 20 min. Finally, the buffer was reintroduced to flush away weakly bound protein for additional 8 min. The protein adsorption quantity was obtained by correlating to the relation of 120 m° in the angle shift of SPR (Δq_{SPR}) equal to a change in protein density of $100\,ng/cm^2$ according to the manufacturer's instruction.

2.5. Fib conformation and activity on DOF surface

GIR spectroscopy was used to determine the conformational state of adsorbed Fib. DOF coated gold-film glass slides were incubated in 1 mg/mL Fib solution for 1 h, rinsed in deionized water, and dried with nitrogen stream. GIR spectra were recorded in the range of $500–4000\,cm^{-1}$. The amide I band, in the range of $1600–1700\,cm^{-1}$ composed of the absorptions of various secondary structural elements of a protein [25], was decomposed into the corresponding peaks by curve-fitting for conformation analysis. Curve-fitting was performed using the associated OPUS spectroscopy software. The peak positions of individual element bands were assigned using the reported data [25]. The activity of the adsorbed Fib was determined using an electrochemical ELISA method [26].

3. Results and discussion

3.1. Synthesis and characterization of polymers

Three terpolymers and one control without F component were obtained by the random free-radical polymerization of the three monomers (D, O, and F) in varying ratios (Scheme 1). The polymerization was carried in DMF at 65 °C for 12 h and the polymers were easily purified by precipitation in diethyl ether to give good yields (~60%). The polymerization was facile despite in the presence of catechol moiety, a polyphenol structure that has been conventionally considered a radical scavenger. The reason that is able to polymerize in this condition is not fully understood at present, but it really worked to give copolymers with molecular weights not so high. Similar works using the unprotected dopaimine moieties in construction of acrylic copolymers via free radical polymerization have also been demonstrated by Lee [27] and Han [28]. The polymer structures were confirmed using FT–IR, ^1H NMR, and GPC. The FT–IR spectra indicate the presence of the three monomeric functionalities in terpolymer as compared to that of their respective monomers (Fig. S1). The ^1H NMR spectra of the copolymers (Fig. S2) were used to calculate the relative abundances of individual monomers. The relative contents of monomers D and O in polymer were determined by integrating the characteristic resonance peaks of Ph-H at 6.82 and 6.58 ppm for D, CH_3-O at 3.36 ppm for O; while the relative amount of F was determined by subtracting the calculated abundance of O in the range of 4.00–4.50 ppm to yield the characteristic absorption abundance of COO-CH_2 in F. One copolymer was determined to have the molar ratio of 1:6:12, giving a formula denoted as DOF1612. Using the same method, the other two terpolymers and the control polymer were determined to have the formulas denoted as DOF495, DOF164, and DOF250, respectively, with the latter having no F pendant in the polymer. The results are summarized and shown in Table 1, along with the molecular weights determined by GPC (Table 1 and Fig. S3).

The molecular weights of the copolymers obtained by GPC measurement are in the range of 15–20 kDa, and because the individual molecular weights for D, O, and F are 221, 275, and 418, respectively, it is expected that these polymers have lengths of ~50 units in the polymer chain with the D unit content ranging from 9.1 to 22 mol%. The contents of D unit in these polymers are comparable to that in the adhesive copolymers previously reported (11–12 mol%) [28]. The ratio of the three monomers in copolymer can be tuned easily by varying the employed amounts of the three monomers in polymerization, even though they may have different competitive rates. For example, in the synthesis of DOF1612, the employed molar ratio was 1:3:6, implying that the monomer D has a lower competitive rate; however, if the content of D in the polymerization solution was raised, a higher content of D resulted in the polymer, such as in the preparation of high dopamine-containing DOF495. Importantly, the copolymers are poorly soluble in diethyl ether but have good solubility in a number of other organic solvents such as CH_2Cl_2, THF, methanol, etc. The solubility difference in organic solvents benefits the precipitation purification process, the ^1H NMR characterization in $CDCl_3$, the GPC test in THF, and the convenient coating preparation by casting the solution on various solid surfaces.

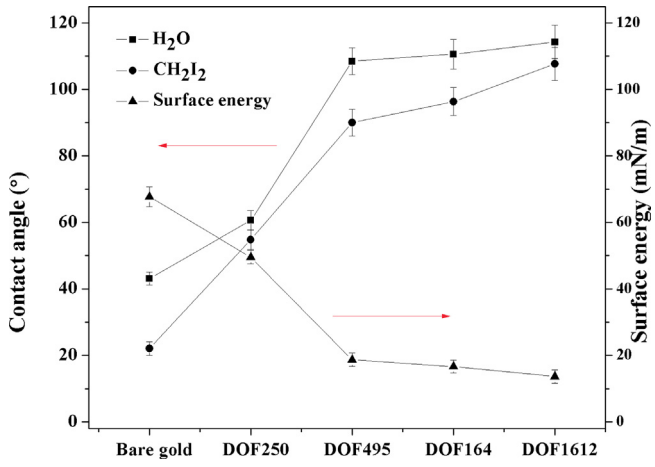

Fig. 1. Static contact angles surface energies of DOF coatings as a function of composition.

3.2. Characterization of polymer coatings

The polymers are endowed with the ability to form coatings on virtually any surface as a result of the adhesive catechol moieties. Due to the amphiphilic nature of the polymers, the surface wettability is a key parameter to characterize their coatings. Fig. 1 shows the static contact angles of water and CH_2I_2 and the surface energies of DOF coated surfaces along with the control bare gold surface.

The bare gold surface has low contact angles to both water and diiodomethane droplets and thus is a surface of high surface energy. After coating with polymers, the increase in contact angle and the decrease in surface energy are obvious. The DOF250 surface, which has no F component, exhibits contact angles nearly 60° for water and 55° for CH_2I_2. This polymer is anticipated to give a surface comprising of pure OEG segments at the air/coating interface, and the water contact angle is in agreement with the typical value of 64° for the coating surface of catechol-based grafted PEG [20]. For coatings of the three terpolymers, the surfaces have much higher static water contact angles in the range from 95° to 115° and much lower surface energies, indicating that they are hydrophobic surfaces, similar to the reported values of fluoropolymer-poly(ethyleneglycol) composite coatings [13]. Accordingly, the CH_2I_2 contact angles are between 92° and 107°, indicating an amphiphobic nature under air. The stability of these coatings was also tested preliminarily by contact angle measurements before and after immersion in different solvents including water, ethanol, and DMF for 1 day (Table S1). No significant change in contact angle was found, manifesting these coatings are resistant to solvents and have good stability.

During the water contact angle measurements, a phenomenon concerning the water contact angle change was observed on freshly prepared coatings. The water contact angle on the DOF495 coating rapidly decreased from the initial 108° to 63° in 10 s, and that on the DOF164 coating changed from 110° to 65°, whereas the DOF1612 coating did not show any change. For CH_2I_2 contact angle, all surfaces gave no change (Fig. S4). Note that the F fractions in these terpolymers are 27.8, 36.4, and 63.2 mol%, respectively, meaning more the F fraction, less the change on water contact angle occurred over time. This phenomenon has been observed by Brown et al. in the coating of amphiphilic fluorosurfactant-grafted poly(styrene—maleic anhydride) [29], but no report on the effect of F content variation on water contact angle. The fast transition of surface wettability from hydrophobic to hydrophilic likely comes from the interface reconstruction/chain reorganization when the interface is changed from air/polymer to water/polymer [29]. The interface reconstruction is closely related to the surface F fraction, and the higher F fraction in the DOF1612 interface is likely to prevent this process. Interestingly, the transition in contact angle was able to be repeated only less than 5 times, and thereafter the contact angle became constant as the initial values as shown in Fig. 1. The underlying mechanism of this process is not understood at present but possibly related to the interface reconstruction and self-assembling process of the polymer coatings.

The grazing incidence FT–IR (GIR) spectra of the DOF coatings by spin-coating on gold substrate in the interested bands of 800–1900 and 2700–3100 cm^{-1} are shown in Fig. 2. All the coatings have characteristic adsorptions of around C=O (1750 cm^{-1}) and CH_2 (2930–2870 cm^{-1}). For the DOF250 coating, the strong peak at around 1110 cm^{-1} assigned to the asymmetric —C—O—C— stretching [30] of monomer OEG is clearly present, which becomes less intensive with the increase of F fraction (curves b–d in Fig. 2). For the coatings of the three terpolymers, they have similar IR absorption patterns (Fig. 2b–d). The two characteristic peaks of C—F stretching locate at 1143 (A_1) and 1240 (A_2) cm^{-1}, respectively, and the ratio of the two peak areas (A_1/A_2) corresponds to that of the perpendicular over the parallel dipole moments in the stretching vibration of CF_2, thus a smaller ratio suggests a more vertical orientation of the chain axis of the F fraction on the surface [31]. The highest ratio was found for the DOF164 (36.4 mol% F) coating, revealing the chain orientation more parallel to the surface; whereas the decrease (DOF495, 27.8 mol% F) or increase (DOF1612, 63.2 mol% F) of F fraction would result in the chain orientation more vertical to the surface. In addition, the absorption peak intensities (A_1 and A_2) of CF_2 stretching increase with the increase of F fraction in the coatings (Fig. 2b–d).

DOF coatings were also characterized by XPS, and the high-resolution spectra of C1s and F1s are given in Fig. 4. The DOF250 surface displays the only characteristic C1s binding energy (BE) at 284.9 eV, whereas the DOF surfaces containing F constituent show three C1s peaks, around at 284.7, 290.6, and 293.1 eV (Fig. 3a), representing the BEs of C1s from CH_2, CF_2, and CF_3 groups, respectively [26]. In Fig. 3b, the F1s BE of the DOF surfaces appears at 686.5 eV for DOF495 and DOF164, and shifts up to 687.5 eV for the DOF1612 surface. Similar BE shifts of C1s and F1s in XPS spectra were observed by Ballav et al. for the partially fluorinated alkanethiols self-assembled monolayers, and ascribed to the effect of dipole alignment on the work function of the XPS photoemission process [32]. In agreement with the expectation, the peak intensities at the BEs of C1s of CF_2 and F1s are substantially increasing with the increase of F fraction in coating.

Owing to the low surface energy nature, the migration and enrichment of fluorinated segments in coating may occur [33]. In the present study, the fluorine atom concentration percentages for the polymers of DOF495, DOF164, and DOF1612 were calculated to be 17.8, 22.4, and 33.3 mol%, respectively, in bulk. After coating, the concentrations were measured to be 25.4, 31.7, and 42.6 mol%, corresponding to the increases by 42.7%, 41.5%, and 27.9%, respectively. The increases reveal the migration and enrichment of the perfluoroalkyl segments at the air/coating interface, and more importantly, the less the F fraction in the polymeric bulk, the larger the enrichment effect is, showing a typical surface energy-driven process.

To investigate the surface morphology of the polymer coatings, AFM images were acquired on each surface of the polymer coatings on silicon substrate (3D images in Fig. 4 and 2D images plus silicon wafer images in Fig. S5). It is seen clearly that the morphologies varies dramatically depending on the polymer structure. The coating of DOF250, which has no F component, consists of mainly large aggregates associated with some small domains. The DOF495 coating is comprised of evenly and densely distributed domains of average size 100 nm. Evenly distributed large domains of average size 400 nm can be seen on the DOF164 coating. For the coating of DOF1612, it is constituted of unevenly distributed domains with

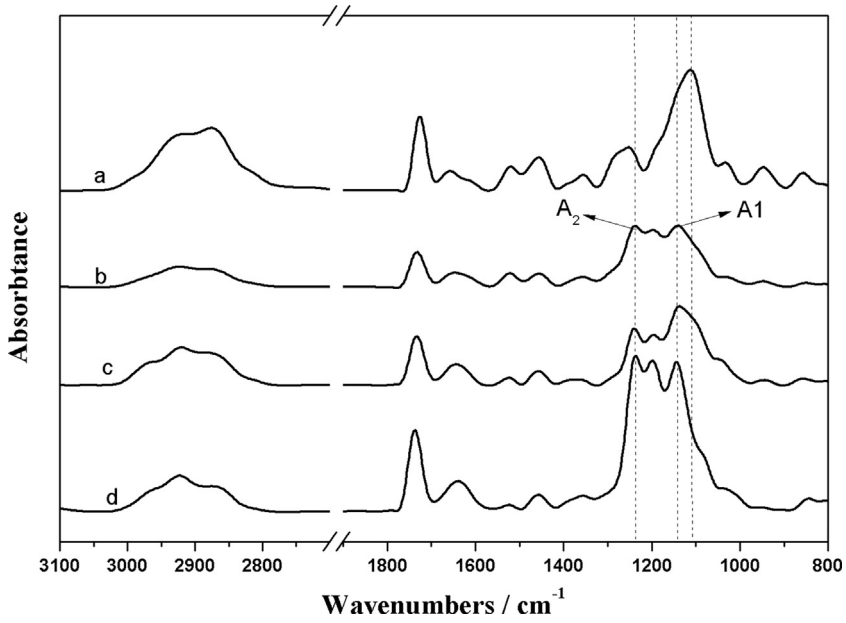

Fig. 2. GIR spectra of DOF coatings: (a) DOF250, (b) DOF495, (c) DOF164, and (d) DOF1612. The bands A_1 and A_2 represent the stretching of the perpendicular and parallel dipole moments of CF_2, respectively [31].

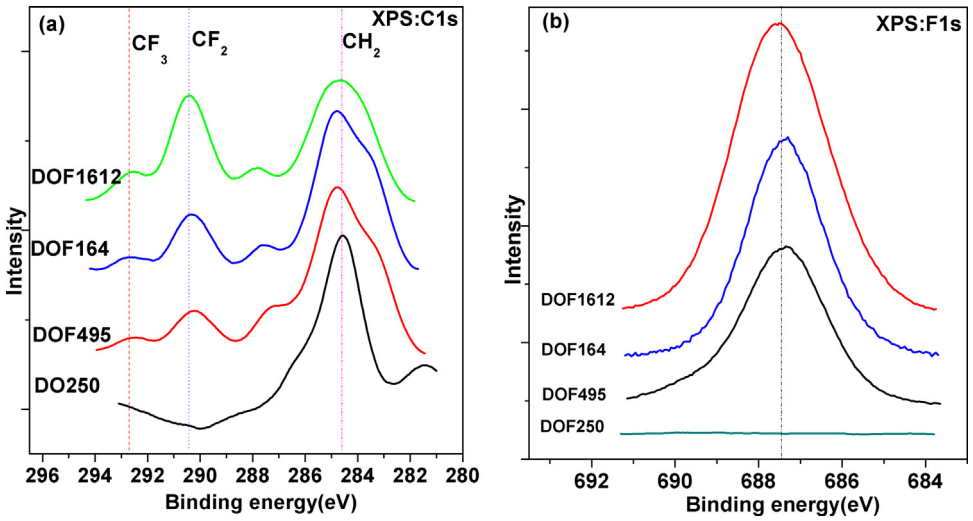

Fig. 3. High-resolution XPS spectra of C1s (a) and F1s (b) of the polymer coatings.

largely varying sizes. Interestingly, a more close inspection reveals that the domains of DOF495 and DOF164 coatings are composed of crater-type self-assembled architectures with open mouth sizes of average 50 nm for the former and 200 nm for the latter; whereas the DOF250 and DOF1612 coatings show only solid domains without any open mouths.

With the data of polymer compositions (Table 1) and the morphologies of these polymer coatings shown here, two preliminary relations can be derived that suggest: (1) catechol moieties enable the amphiphobic coating formation under dip-coating conditions; (2) a rational combination ratio of the individual components dominate the coating surface morphology. The adsorption of catechol-carrying polymers on various surfaces has been well documented, and it is attributed to the complex interface interactions including covalent bonds, hydrogen bonds, strong physical interactions, as well as possibly inter-chain cross-linking of the polymer, to afford robust coatings [20]. The formation of distinctive surface architectures of amphiphilic copolymer coatings are a common phenomenon, which can be related to the nature of hydrophilic and hydrophobic segments depending on their composition ratio [15]. In our case, it is anticipated that not only the hydrophilic and hydrophobic segments but also the catechol moieties play an indispensable role, though the in-depth mechanism is not clear at present.

3.3. Protein adsorption on DOF surfaces

The fouling process of biospecies on a surface is the initial non-specific adsorption of biomacromolecules as the key step to following bacterial attachment [3]. Therefore, using model proteins for assessing the nonfouling properties of a surface is a reliable technique in developing antifouling coatings. Two model proteins, BSA and Fib, were chosen for this purpose and their adsorption on the DOF surfaces was characterized by SPR. The adsorption of Fib on the DOF surfaces is exemplarily shown in Fig. 5a, where it is seen that the adsorption capacity follows

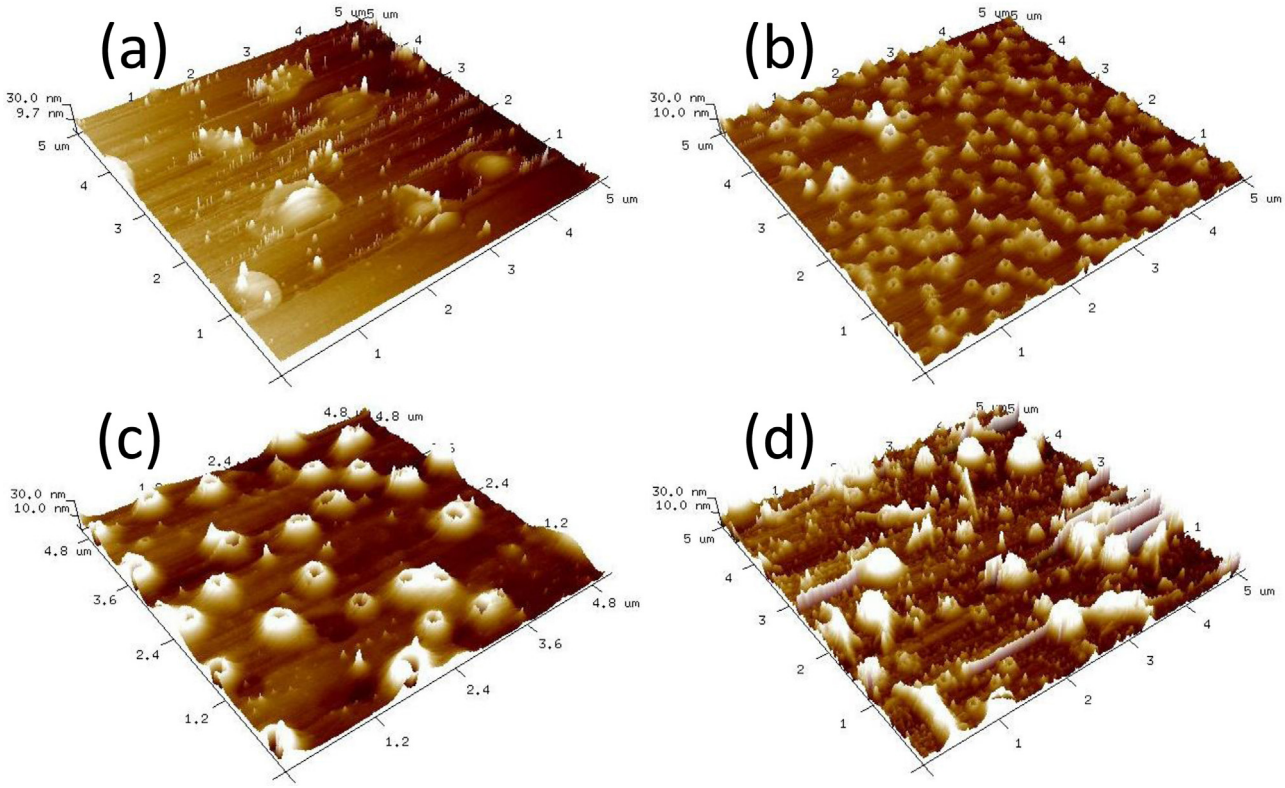

Fig. 4. 3D AFM images of polymer coatings: (a) DOF250, (b) DOF495, (c) DOF164, (d) DOF1612. The scan size is 5 × 5 μm and shown with a fixed height 30 nm for each image.

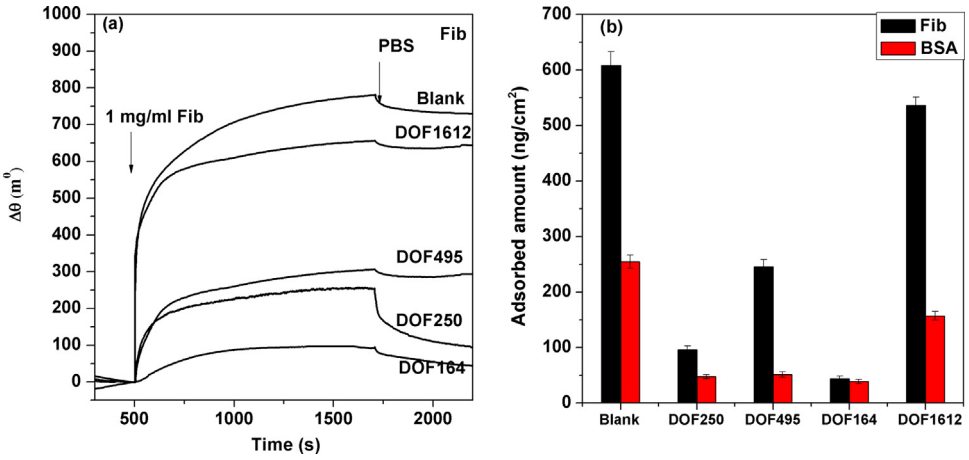

Fig. 5. SPR sensorgrams of Fib adsorption (a) and the comparison of BSA and Fib adsorption amounts (b) on DOF surfaces.

the order: blank gold > DOF1612 > DOF495 > DOF250 > DOF164. The adsorption of BSA gave a similar trend but with much lower capacities as shown in Fig. 5b. The DOF164 surface (36.4 mol% F) has a strong antifouling property with the least adsorption amounts of 43.5 and 38.7 ng/cm^2 for Fib and BSA, respectively; whereas the DOF1612 surface (63.2 mol% F) shows a much higher adsorption level up to 535.5 ng/cm^2 for Fib, 12.3 folds higher as compared to the DOF164 surface. It is worthy of mention that the DOF164 surface has a much lower capacity than the DOF250 surface, which shows an adsorption of 96 ng/cm^2, comparable to a recently reported copolymer P(DMA15-b-PEGMA32) with a capacity of 80 ng/cm^2 [34].

The lowest protein adsorption of the DOF164 surface is an interesting contrast to the highest capacity of the DOF1612 surface, suggesting the importance of F fraction in antifouling copolymers [26]. On the other hand, surface morphology has been reported to have a vital role in controlling protein adsorption [15]. For the protein adsorption on a surface with morphology of partitioned hydrophilic and hydrophobic zones, the adsorption process is likely governed by the attachment of the hydrophobic parts of the protein onto the hydrophobic area of the surface, avoiding the thermodynamically unfavorable dehydration from both the approaching surfaces. Based on this assumption, the mutual matching of the hydrophobic zone sizes, from both the protein and the substrate surfaces, may be critical to the protein adsorption [26]. The hydrophobic area of the DOF164 surface may mismatch whereas that of the DOF1612 surface may match to a greater extent with that of the protein, leading to the highly resistant or highly adsorptive surfaces, respectively.

One advantage of the DOF polymers is their ability to form coatings on virtually any surface, and thus coatings on stainless steel

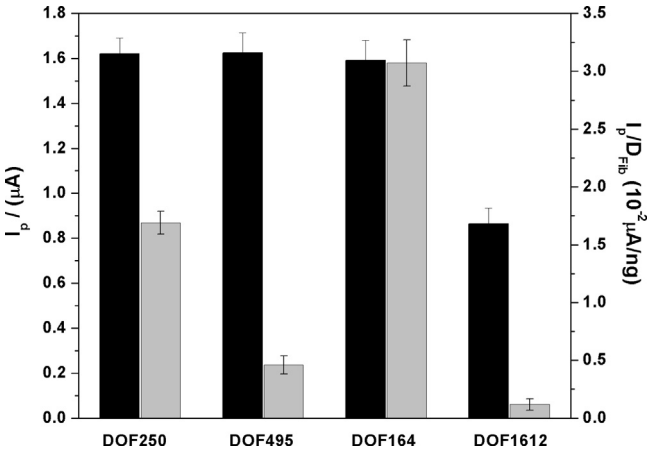

Fig. 6. Electrochemical immunosorbent assays of the total (black columns) and unit (grey columns) activities for Fib adsorbed on the DOF surfaces.

were also prepared for ascertaining the antifouling properties. Fluorescence images were acquired (Fig. S6) after incubation of the substrates in the PBS solution of fluorescein-labeled FITC-Fib. The results showed once again that the DOF164 surface has the least protein adsorption, consistent with the result on gold substrate measured by SPR.

3.4. Conformation analysis and activity of adsorbed Fib

GIR spectroscopy is a useful tool to evaluate the conformational state of surface adsorbed proteins. The interested GIR absorption region from 1200 to 1800 cm^{-1} for Fib adsorbed on DOF surfaces (Fig. S7a) can be used to analyze the secondary element composition of the protein structure [35]. The typical amide absorption bands at around 1665 (amide I), 1545 (amide II), and 1247 cm^{-1} (amide III) were clearly present. The most meaningful amide I band can be decomposed into several peaks by curve-fitting, corresponding to the absorptions of the secondary structural elements including β-turn ($1680 \pm 3\ cm^{-1}$), α-helix ($1658 \pm 1\ cm^{-1}$), random structures ($1648 \pm 2\ cm^{-1}$), and β-sheet ($1633 \pm 2\ cm^{-1}$), as well as the side chain moieties ($1620\ cm^{-1}$) [35] (Fig. S7b–e). The integral intensity ratios of β-sheet/β-turn for adsorbed Fib were calculated to be ca. 1.24, 0.98, 1.69, and 0.68 on the DOF250, DOF495, DOF164, and DOF1612 surfaces, respectively. The integral intensity ratio is a biocompatibility indicator of the surface, and a larger ratio value suggests a more favorable protein conformation in maintaining its activity [35]. Since the DOF164 surface displays the highest β-sheet/β-turn ratio for the adsorbed protein, it is superior in terms of protein compatibility over the other polymer surfaces.

The total and unit activities of adsorbed Fib were also evaluated by electrochemical immunosorbent assays (Fig. 6). The assay was followed a reported method that has been used to probe the availability of the antibody recognizing domains as well as the bioactivity state of an adsorbed protein [36]. The total activities of Fib on DOF250, DOF495, and DOF164 surfaces, except for DOF1612, remain to be similar; however, the unit activities, a ratio of immunoactive response peak current density (Ip, μA/cm^2) over adsorbed Fib amount (D_{Fib}, ng/cm^2), are significantly different. The highest unit activity, 3.07×10^{-2} μA/ng was found for Fib adsorbed on the DOF164 surface. For the DOF1612 surface, although it has a highest capacity of Fib adsorption (535.5 ng/cm^2), the total and unit activities are the lowest (0.864 μA and 0.12×10^{-2} μA/ng, respectively). The least protein adsorption capacity but with the highest unit protein activity for Fib on the DOF164 surface implies the surface is highly protein compatible. On the other hand, the DOF1612 surface has the highest protein adsorption capacity but shows the least unit protein activity, suggesting most protein molecules adsorbed on the surface were in a denatured state, which can also be inferred from the lowest β-sheet/β-turn ratio of 0.68 in GIR characterization (Fig. S7e).

Protein compatibility is a conventional but still challenging concern in biomaterial design up to now [37]. The concept, protein compatibility, generally refers to the ability of a material surface not only to adsorb lower amounts of protein but also to lower the potential for protein denaturation upon attachment [35]. PEGs are well-known and widely used biomaterials due to their high protein compatibility. The PEG-like DOF250 surface shows a low amount of protein adsorption but with a high unit activity as compared to the DOF495 and DOF1612 surfaces, manifesting the good protein compatibility of DOF250. Nevertheless, DOF250 is inferior to DOF164 in terms of the low protein adsorption and non-denaturing property, with protein adsorption capacity of 96 versus 43 ng/cm^2 and unit activity of 1.69×10^{-2} versus 3.07×10^{-2} μA/ng. The lower protein adsorption capacity of the DOF164 surface may be attributed to the distinct morphology unfavorable toward protein adsorption [15] as discussed above. The stabilization of protein secondary structural element and the preservation of activity upon adsorption on the DOF164 surface are intriguing and cannot be given a reasonable explanation at present, though a recent report demonstrated that the perfluoroalkyl surface can be used for protein immobilization without causing significant denaturation [38]. Therefore, it is worthy of further investigation.

4. Conclusions

In this study, terpolymers with pendant catechol, OEG and perfluoroalkyl functional groups in varying ratios were synthesized and used to prepare antifouling coatings. The catechol moieties promoted the polymers to form stable coatings onto substrate surfaces, whereas the OEG and perfluoroalkyl segments in an appropriate ratio enhanced the antifouling ability of the coatings. Special phenomena such as the fast surface wettability transition from hydrophobic to hydrophilic and the self-assembly into crater-type aggregates were found and discussed in terms of the terpolymer composition. It was preliminarily concluded that the F content and the subsequent self-assembled morphology, instead of the surface energy, determined the surface protein adsorption capacity. The DOF164 surface exhibited the excellent antifouling ability and meanwhile the stabilization ability to protein conformation, leading to a protein activity even better than the protein compatible OEG surface. The features of low protein adsorption but high protein activity preservation as well as the ability to form coatings on virtually any surface render the terpolymer DOF164 with the potential to be utilized in biomaterial development.

Acknowledgements

This work is supported by the Hubei Provincial Natural Science Foundation (2013CFB24) and in part by the Natural Science Foundation of China (21172087 and 21472064).

Appendix A. Supplementary data

Supplementary data associated with this article can be found, in the online version, at http://dx.doi.org/10.1016/j.colsurfb.2015.12.051.

References

[1] B. Indrani, R.C. Pangule, R.S. Kane, Antifouling coatings: recent developments in the design of surfaces that prevent fouling by proteins, bacteria, and marine organisms, Adv. Mater. 23 (2011) 690–718.

[2] A. Hucknall, S. Rangarajan, A. Chilkoti, In pursuit of zero: polymer brushes that resist the adsorption of proteins, Adv. Mater. 21 (2009) 2441–2446.
[3] J.L. Harding, M.M. Reynolds, Combating medical device fouling, Trends Biotechnol. 32 (2014) 140–146.
[4] D. Rana, T. Matsuura, Surface modifications for antifouling membranes, Chem. Rev. 110 (2010) 2448–2471.
[5] J. Xu, D.A. Bohnsack, M.E. Mackay, K.L. Wooley, Unusual mechanical performance of amphiphilic crosslinked polymer networks, J. Am. Chem. Soc. 129 (2007) 506–507.
[6] Y. Chang, Y.J. Shih, C.Y. Ko, J.F. Jhong, Y.L. Liu, T.C. Wei, Hemocompatibility of poly(vinylidene fluoride) membrane grafted with network-like and brush-like antifouling layer controlled via plasma-induced surface pegylation, Langmuir 27 (2011) 5445–5455.
[7] C.J. Weinman, N. Gunari, S. Krishnan, R. Dong, M.Y. Paik, K.E. Sohn, G.C. Walker, E.J. Kramer, D.A. Fischer, C.K. Ober, Protein adsorption resistance of anti-biofouling block copolymers containing amphiphilic side chains, Soft Matter 6 (2010) 3237–3243.
[8] J. Zheng, W. Song, H. Huang, H. Chen, Protein adsorption and cell adhesion on polyurethane/pluronic surface with lotus leaf-like topography, Colloids Surf. B: Biointerfaces 77 (2010) 234–239.
[9] J.B. Schlenoff, Zwitteration: coating surfaces with zwitterionic functionality to reduce nonspecific adsorption, Langmuir 30 (2014) 9625–9636.
[10] C. Perrino, S. Lee, S.W. Choi, A. Maruyama, N.D. Spencer, A biomimetic alternative to poly(ethylene glycol) as an antifouling coating: resistance to nonspecific protein adsorption of poly(L-lysine)-graft-dextran, Langmuir 24 (2008) 8850–8856.
[11] E. Martinelli, E. Guazzelli, C. Bartoli, M. Gazzarri, F. Chiellini, G. Galli, M.E. Callow, J.A. Callow, J.A. Finlay, S. Hill, Amphiphilic pentablock copolymers and their blends with PDMS for antibiofouling coatings, J. Polym. Sci. Part A: Polym. Chem. 53 (2015) 1213–1225.
[12] R.B. Bodkhe, S.J. Stafslien, J. Daniels, N. Cilz, A.J. Muelhberg, S.E.M. Thompson, M.E. Callow, J.A. Callow, D.C. Webster, Zwitterionic siloxane-polyurethane fouling-release coatings, Prog. Org. Coat. 78 (2015) 369–380.
[13] C.S. Gudipati, J.A. Finlay, J.A. Callow, M.E. Callow, K.L. Wooley, The antifouling and fouling-release perfomance of hyperbranched fluoropolymer (HBFP)-poly(ethyleneglycol) (PEG) composite coatings evaluated by adsorption of biomacromolecules and the green fouling *Alga Ulva*, Langmuir 21 (2005) 3044–3053.
[14] W. van Zoelen, H.G. Buss, N.C. Ellebracht, N.A. Lynd, D.A. Fischer, J. Finlay, S. Hill, M.E. Callow, J.A. Callow, E.J. Kramer, R.N. Zuckermann, R.A. Segalman, Sequence of hydrophobic and hydrophilic residues in amphiphilic polymer coatings affects surface structure and marine antifouling/fouling release properties, ACS Macro Lett. 3 (2014) 364–368.
[15] J.L. Kerstetter, W.M. Gramlich, Nanometer-scale self-assembly of amphiphilic copolymers to control and prevent biofouling, J. Mater. Chem. B 2 (2014) 8043–8052.
[16] P. Murugan, M. Krishnamurthy, S.N. Jaisankar, D. Samanta, A.B. Mandal, Controlled decoration of the surface with macromolecules: polymerization on a self-assembled monolayer (SAM), Chem. Soc. Rev. 44 (2015) 3212–3243.
[17] H.-X. Wu, L. Tan, M.-Y. Yang, C.-J. Liu, R.-X. Zhuo, Protein-resistance performance of amphiphilic copolymer brushes consisting of fluorinated polymers and polyacrylamide grafted from silicon surfaces, RSC Adv. 5 (2015) 12329–12337.
[18] Q. Ye, F. Zhou, W. Liu, Bioinspired catecholic chemistry for surface modification, Chem. Soc. Rev. 40 (2011) 4244–4258.
[19] H. Lee, S.M. Dellatore, W.M. Miller, P.B. Messersmith, Mussel-inspired surface chemistry for multifunctional coatings, Science 318 (2007) 426–430.
[20] Q. Wei, T. Becherer, P.-L.M. Noeske, I. Grunwald, R. Haag, A universal approach to crosslinked hierarchical polymer multilayers as stable and highly effective antifouling coatings, Adv. Mater. 26 (2014) 2688–2693.
[21] L. Ma, H. Qin, C. Cheng, Y. Xia, C. He, C. Nie, L. Wang, C. Zhao, Mussel-inspired self-coating at macro-interface with improved biocompatibility and bioactivity via dopamine grafted heparin-like polymers and heparin, J. Mater. Chem. B 2 (2014) 363–375.
[22] D. Hong, K. Bae, S.-P. Hong, J.H. Park, I.S. Choi, W.K. Cho, Mussel-inspired, perfluorinated polydopamine for self-cleaning coating on various substrates, Chem. Commun. 50 (2014) 11649–11652.
[23] Q. Wei, T. Becherer, R.-C. Mutihac, P.-L.M. Noeske, F. Paulus, R. Haag, I. Grunwald, Multivalent anchoring and cross-linking of mussel-inspired antifouling surface coatings, Biomacromol 15 (2014) 3061–3071.
[24] H. Xu, J. Nishida, W. Ma, H. Wu, M. Kobayashi, H. Otsuka, A. Takahara, Competition between oxidation and coordination in cross-linking of polystyrene copolymer containing catechol groups, ACS Macro Lett. 1 (2012) 457–460.
[25] S. Tunc, M.F. Maitz, G. Steiner, L. Vazquez, M.T. Pham, R. Salzer, In situ conformational analysis of fibrinogen adsorbed on Si surfaces, Colloids Surf. B: Biointerfaces 42 (2005) 219–225.
[26] S. Li, D. Yang, H. Tu, H. Deng, D. Du, A. Zhang, Protein adsorption and cell adhesion controlled by the surface chemistry of binary perfluoroalkyl/oligo(ethylene glycol) self-assembled monolayers, J. Colloid Interface Sci. 402 (2013) 284–290.
[27] H. Lee, B.P. Lee, P.B. Messersmith, A reversible wet/dry adhesive inspired by mussels and geckos, Nature 448 (2007) 338–341.
[28] H. Han, J. Wu, C.W. Avery, M. Mizutani, X. Jiang, M. Kamigaito, Z. Chen, C. Xi, K. Kuroda, Immobilization of amphiphilic polycations by catechol functionality for antimicrobial coatings, Langmuir 27 (2011) 4010–4019.
[29] P.S. Brown, O.D.L.A. Atkinson, J.P.S. Badyal, Ultrafast oleophobic–hydrophilic switching surfaces for antifogging, self-cleaning, and oil–water separation, ACS Appl. Mater. Interfaces 6 (2014) 7504–7511.
[30] R. Valiokas, S. Svedhem, S.C.T. Svensson, B. Liedberg, Self-assembled monolayers of oligo(ethylene glycol)-terminated and amide group containing alkanethiolates on gold, Langmuir 15 (1999) 3390–3394.
[31] R. Colorado, M. Graupe, O.E. Shmakova, R.J. Villazana, T.R. Lee, Interfacial properties on the submicron scale, in: ACS Symposium Series 781, American Chemical Society Washington, DC, 2001, pp. 276–292.
[32] N. Ballav, A. Terfort, M. Zharnikov, Mixing of nonsubstituted and partly fluorinated alkanethiols in a binary self-assembled monolayer, J. Phys. Chem. C 113 (2009) 3697–3706.
[33] L. Yi, X. Meng, X. Tian, W. Zhou, R. Chen, Wettability of electrospun films of microphase-separated block copolymers with 3,3,3-trifluoropropyl substituted siloxane segments, J. Phys. Chem. C 118 (2014) 26671–26682.
[34] N. Patil, C. Falentin-Daudré, C. Jérôme, C. Detrembleur, Mussel-inspired protein-repelling ambivalent block copolymers: controlled synthesis and characterization, Polym. Chem. 6 (2015) 2919–2933.
[35] G. Steiner, S. Tunc, M. Maitz, R. Salzer, Conformational changes during protein adsorption. FT–IR spectroscopic imaging of adsorbed fibrinogen layers, Anal. Chem. 79 (2007) 1311–1316.
[36] T.P. Ugarova, C. Zamarron, Y. Veklich, R.D. Bowditch, M.H. Ginsberg, J.W. Weisel, E.F. Plow, Conformational transitions in the cell binding domain of fibronectin, Biochemistry 34 (1995) 4457–4466.
[37] N. Hammer, F.P. Brandl, S. Kirchhof, V. Messmann, A.M. Goepferich, Protein compatibility of selected cross-linking reactions for hydrogels, Macromol. Biosci. 15 (2015) 405–413.
[38] H.M. Rapp, S. Bacher, A. Ahrens, W. Rapp, B. Kammerer, G.U. Nienhaus, W. Bannwarth, Attachment of proteins to surfaces by fluorous–fluorous interactions restoring their structure and activity, ChemPlusChem 77 (2012) 1066–1070.